

Complex permittivity of the deuterated and undeuterated proton glass $\text{Rb}_{1-x}(\text{NH}_4)_x\text{H}_2\text{AsO}_4$

F. L. Howell,* N. J. Pinto, and V. H. Schmidt

Department of Physics, Montana State University, Bozeman, Montana 59717

(Received 27 January 1992; revised manuscript received 1 June 1992)

Dielectric measurements have been performed in both the deuterated and undeuterated proton glass rubidium ammonium dihydrogen arsenate $\text{Rb}_{1-x}(\text{NH}_4)_x\text{H}_2\text{AsO}_4$ along the tetragonal a axis. Ammonium concentrations x of 0, 0.01, 0.05, and 0.10 were studied for the undeuterated sample, while ammonium concentrations of 0, 0.05, and 0.10 were studied for the deuterated counterpart. Glassy behavior is present for $x=0.05$ and 0.10 but could not be observed for lower ammonium concentrations. For $x=0.05$ and 0.10 we observed coexistence of paraelectric or proton-glass and ferroelectric order below the "glass transition" temperature T_g due to the random spatial fluctuations of the ammonium cation. Cole-Cole plots for the $x=0.10$ sample show that there is a distribution of relaxation times below T_g . This relaxation occurs in the proton-glass portion of the crystal. The activation energies corresponding to these relaxation processes are calculated.

INTRODUCTION

The study of proton glass has received considerable attention during the past decade. Since its discovery by Courtens¹ in $\text{Rb}_{1-x}(\text{NH}_4)_x\text{H}_2\text{PO}_4$ (RADP) many experiments have been carried out²⁻⁵ on crystals with various ammonium concentrations x in an attempt to construct the phase diagram. Such a diagram shows the boundaries between the paraelectric (PE) and ferroelectric (FE) phases for small ammonium (x) concentrations and the boundary between the PE and antiferroelectric (AFE) phase for large- x values. Many⁶⁻¹⁵ experimental and theoretical studies have also been done on the proton glass $\text{Rb}_{1-x}(\text{NH}_4)_x\text{H}_2\text{AsO}_4$ (RADA). Microwave dielectric measurements on RADA by Trybula *et al.*¹⁴ showed that the phase diagram is asymmetric, which is partly due to the difference in the transition temperatures of the pure constituents.

Spin-glass and pseudo-spin-glass behavior is generally considered to require randomness and frustration. In proton glass the randomness lies in the Rb^+ and NH_4^+ cation placement. The frustration lies in two inconsistent tendencies for ordering of the $\text{O-H}\cdots\text{O}$ proton "pseudospins." In ferroelectric RbH_2AsO_4 (RDA) if one looks down along c , the protons in $\text{O-H}\cdots\text{O}$ bonds lying along a (b) are near the tops (bottoms) of AsO_4 groups, or *vice versa* for reversed domains. In antiferroelectric $\text{NH}_4\text{H}_2\text{AsO}_4$ (ADA) two adjacent $\text{N-H}\cdots\text{O}$ bonds (viewed along c) of a given NH_4^+ ion are short and the other two adjacent $\text{N-H}\cdots\text{O}$ bonds are long. A given $\text{O-H}\cdots\text{O}$ bond shares oxygens with one short and one long $\text{N-H}\cdots\text{O}$ bond, with O-H near the long bond and the $\text{H}\cdots\text{O}$ near the short bond. This arrangement puts one proton near the top and one near the bottom of each AsO_4 group, which is inconsistent with ferroelectric ordering. In a mixed crystal, these inconsistent ordering schemes favored by the arsenate and ammonium ions cause frustration and inhibit or prevent either ferroelectric or antiferroelectric ordering.

The proton-glass state for the RADA system exists in the concentration range $0.04 < x < 0.50$. The first set of dielectric measurements on RADA for $x=0.35$ was reported by Kim, Kim, and Lee.¹³ Their data, which extend down to 20 K, did not show any onset of proton-glass behavior for permittivity along the a axis. Subsequent measurements on RADA for the same x value by Trybula *et al.*¹¹ do show the onset of proton-glass behavior with glass transition temperatures ranging from 38 to 28 K for ac excitation frequencies of 30 kHz down to 1 Hz, respectively. Additional dielectric measurements on RADA for $0.10 < x < 0.20$ (Refs. 6 and 7) also show the existence of proton-glass behavior and the suggested phase diagram. While these experiments concentrated on x values near the ferroelectric to proton-glass phase boundary, in this paper we present our dielectric investigations in RADA and DRADA (deuterated) mixed crystals with lower x values away from this boundary and show the coexistence of proton-glass and ferroelectric order.

EXPERIMENT

Mixed crystals of RADA for all the ammonium concentrations reported here were obtained by slow evaporation of aqueous solutions of RbH_2AsO_4 and $(\text{NH}_4)\text{H}_2\text{AsO}_4$ mixed in the proper molar ratios. The deuterated crystals were grown under an atmosphere of argon to maintain a high percentage of deuteration since the ferroelectric transition temperature is sensitive to the degree of deuteration of the crystal. The x values are obtained to within 10% with the aid of phase diagrams for RADA (Refs. 7 and 9) samples and to within 15% with the aid of the phase diagram for DRADA (Ref. 10) samples. The larger uncertainty in the deuterated samples is due to the fact that the phase diagram is concentration dependent since the ferroelectric transition temperatures depend upon the percent of deuteration present in the crystal. Small platelets perpendicular to the a tetragonal axis were cut from single crystals. Conducting silver

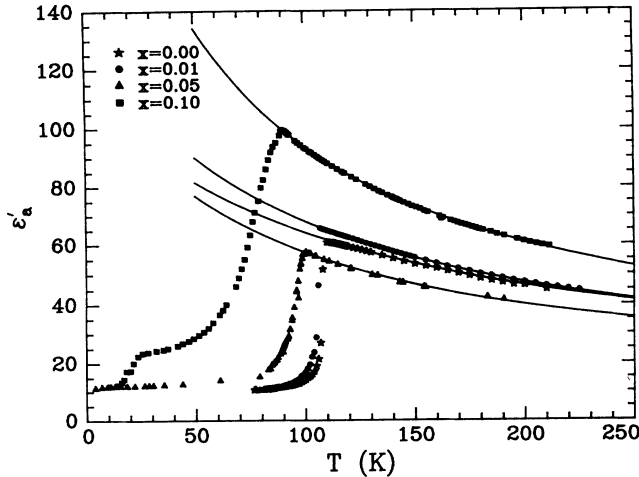


FIG. 1. Temperature dependence of the real part of the dielectric constant ϵ'_a measured along the a axis for various ammonium concentrations x in RADA. The solid line represents a fit to Eq. (1); see Table I for fitting constants.

paint was applied after polishing the surfaces to ensure that faces were parallel. The sample was then placed in a closed copper container. A type-K Chromel-Alumel thermocouple in good thermal contact with the sample was used to measure the temperature. The complex dielectric constant $\epsilon'_a - i\epsilon''_a$ was measured using a General Radio Bridge and a Wayne-Kerr model 6425 Component Analyzer.

RESULTS AND DISCUSSION

Figure 1 shows the temperature dependence of the real part of the dielectric constant ϵ'_a for various values of ammonium concentration x . Figure 2 represents the same but for the deuterated counterpart. Both these figures represent data taken at 1 kHz. For certain x values there are two transitions as evident from the graphs. The first transition (T_c) on lowering the temperature corresponds to the ferroelectric transition and the second "transition" (T_g) at still lower temperature is the proton-glass transition. This "transition" temperature is frequency dependent and is defined as the temperature at which ϵ'_a begins to drop more rapidly with decreasing temperature for that frequency. Table I summarizes the transition temperatures for various x values at 1 kHz. In the RADA sample for $x=0.01$, the dielectric constant ϵ'_a falls to 9 below T_c . This is also the value for ϵ'_a for the pure

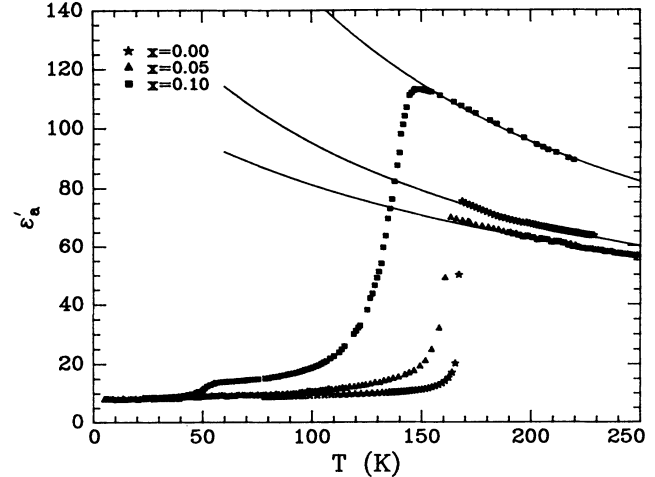


FIG. 2. Temperature dependence of the real part of the dielectric constant ϵ'_a measured along the a axis for various ammonium concentrations x in DRADA. The solid line represents a fit to Eq. (1); see Table I for fitting constants.

($x=0$) sample below T_c , thus ruling out the possibility of observing a glass transition. The sharper drop in ϵ'_a below T_c for decreasing x is consistent with the almost vertical drop one expects to observe in the pure RDA crystal which undergoes a first-order transition^{16,17} at T_c .

Interesting effects are observed upon deuteration. The transition temperatures are significantly increased as can be seen in Table I by comparing the transition temperatures of the deuterated and undeuterated samples with similar x values. These results reflect the greater asymmetry¹⁸ in the O-D...O bond, a quantum-mechanical effect due to the larger mass of the deuteron as compared to the proton. The value of ϵ'_a at T_c is higher in the deuterated samples. We note that T_c for DRADA $x=0.05$ is closer to that for $x=0$ unlike in the RADA case where T_c for $x=0.05$ is half-way between that of $x=0$ and 0.10. This could be attributed to the uncertainty in x and the lesser deuteration content due to repeated redissolving of the solute in heavy water which was done to obtain good crystals. From Figs. 3 and 4 in the case of the deuterated samples at low temperature ϵ''_a goes to zero well above 0 K, while for the undeuterated crystals it stays above zero, in some cases approaching zero with finite slope as temperature goes to zero.

The dielectric constant ϵ'_a from T_c up towards higher temperatures is found to obey the Curie-Weiss behavior. The solid lines in Figs. 1 and 2 represent fits to the Curie-Weiss formula:

TABLE I. Tabulated temperatures of various transitions mentioned in the text including the activation energies responsible for dielectric relaxation. These results (except for the activation energy) are obtained by analyzing the data taken at 1 kHz.

X	T_c (K)	T_g (K)	Undeuterated				Deuterated					
			$\epsilon'_{a\infty}$	C (K)	T_0 (K)	E_a (meV)	T_c (K)	T_g (K)	$\epsilon'_{a\infty}$	C (K)	T_0 (K)	E_a (meV)
0	110		10	11 100±100	-105±2			7	19 800±300	-125±5		
0.01	107		10	10 500±100	-81±1							
0.05	101	15	10	8 100±200	-71±3		163	56	7	22 500±400	-204±7	99
0.1	90	21	10	12 900±100	-54±1	59	146	57	7	24 700±400	-79±4	104

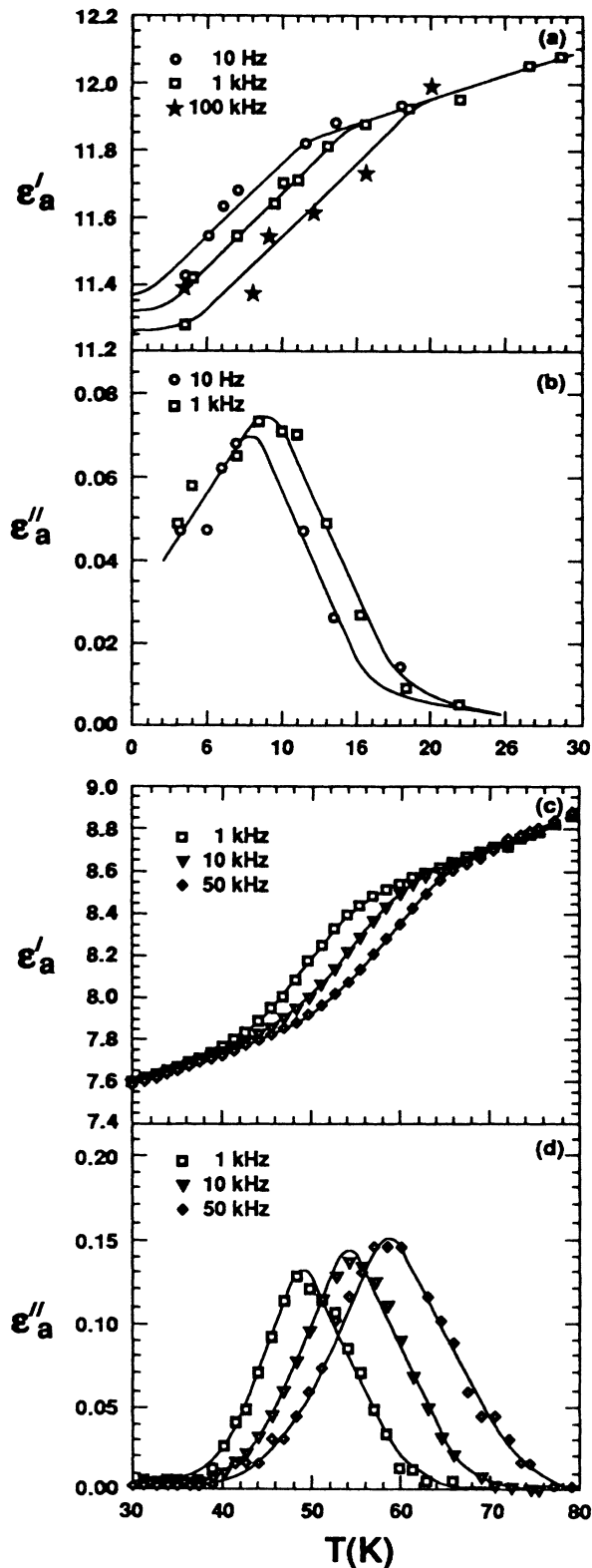


FIG. 3. Temperature dependence of the (a) real part ϵ'_a and (b) imaginary part ϵ''_a of the dielectric permittivity in the proton-glass regime for $x=0.05$ RADA. Temperature dependence of the (c) real part ϵ'_a and (d) imaginary part ϵ''_a of the dielectric permittivity in the proton-glass regime for $x=0.05$ DRADA. The solid lines are guides to the eye.

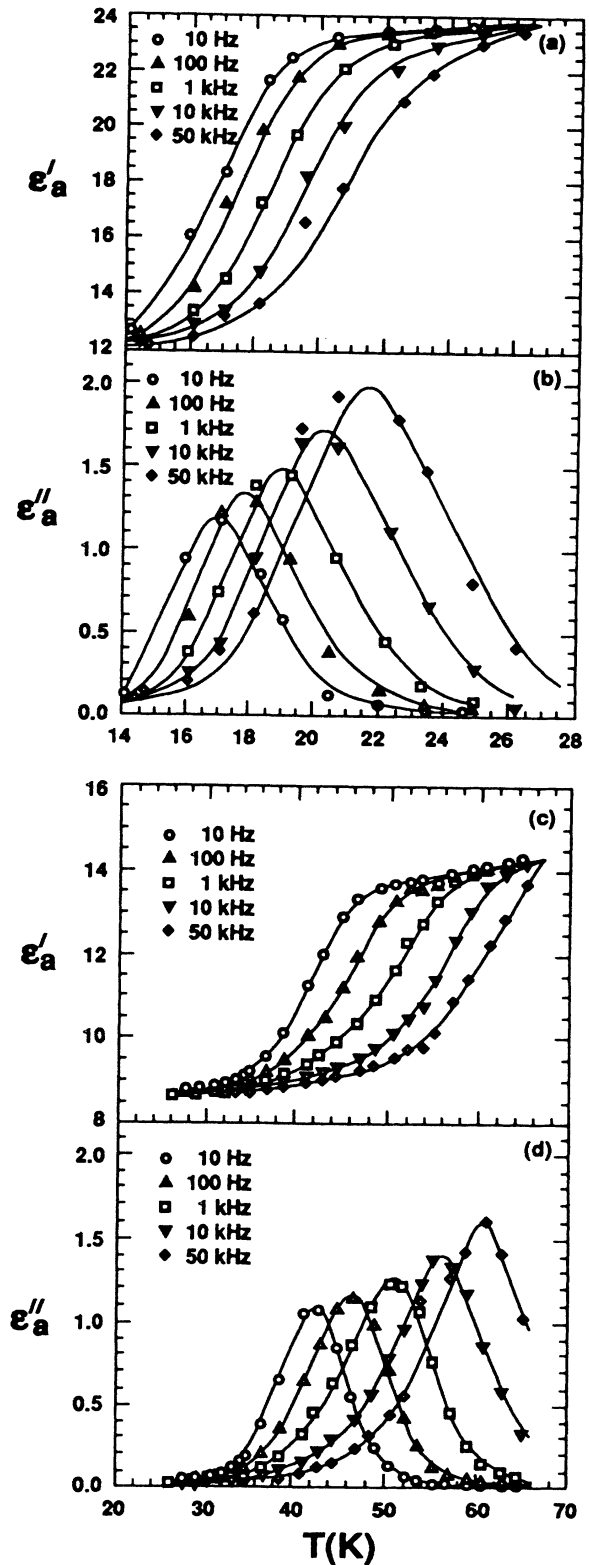


FIG. 4. Temperature dependence of the (a) real part ϵ'_a and (b) imaginary part ϵ''_a of the dielectric permittivity in the proton-glass regime for $x=0.10$ RADA. Temperature dependence of the (c) real part ϵ'_a and (d) imaginary part ϵ''_a of the dielectric permittivity in the proton-glass regime for $x=0.10$ DRADA. The solid lines are guides to the eye.

$$\epsilon'_a - \epsilon'_{a\infty} = C / (T - T_0) \quad (1)$$

where $\epsilon'_{a\infty}$ is the "infinite frequency" dielectric response, C is the Curie-Weiss constant, and T_0 is the Curie-Weiss temperature. Table I shows these fitting parameters for various concentrations x , where the $\epsilon'_{a\infty}$ value is the average of those obtained from Figs. 1, 2, and 5. A similar fit was made² in an RADP sample along the a axis close to the antiferroelectric boundary of the phase diagram. Nagamiya¹⁹ has also made Curie-Weiss fits along the a and c axes in ADP with negative Curie-Weiss temperatures. Essential features of the proton-glass behavior are shown in Figs. 3 and 4. Such behavior at low temperatures is typical for proton glasses in that it shows a dispersion and characteristic maxima of $\epsilon''_a(T)$ a few degrees below the glass transition temperature T_g . The dispersion is greater in the $x=0.10$ samples as compared to the $x=0.05$ samples. We point out that the variation

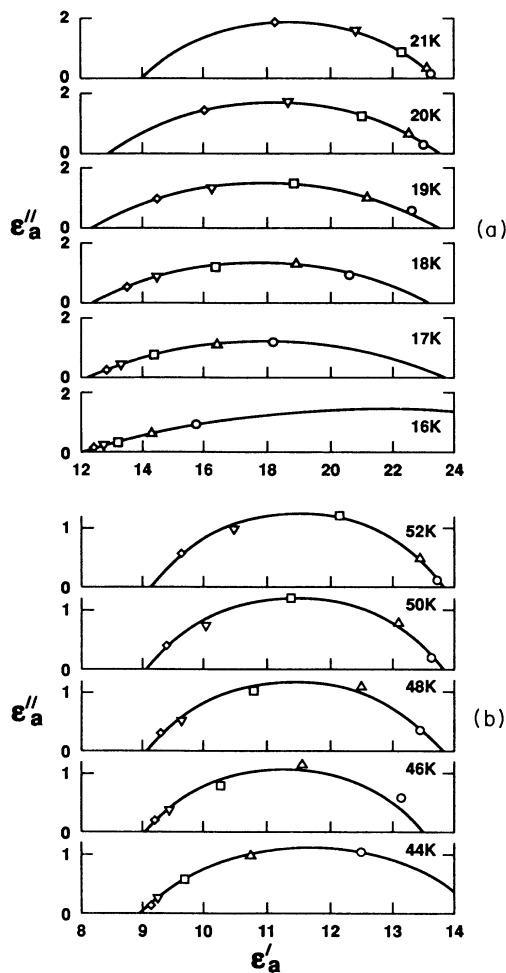


FIG. 5. (a) Cole-Cole plots for $x=0.10$ RADA in the proton-glass region; (b) Cole-Cole plots for $x=0.10$ DRADA in the proton-glass region. The symbols represent the same frequencies as in Fig. 4. The solid lines represent fits to the equation of a circle.

in ϵ''_a in the $x=0.05$ sample Fig. 3(b) is much lower in the undeuterated crystal as compared to the deuterated one Fig. 3(d). It must be noted that we do observe a frequency dependence of ϵ''_a on the low-temperature side of the graph unlike the results of Trybula *et al.*⁷ for $x=0.12$ RADA where the curves all coalesce.

In an attempt to analyze the dielectric relaxation mechanisms below T_g we have constructed Cole-Cole plots for the $x=0.10$ sample from the data shown in Fig. 4. Both plots show that the relaxation processes cannot be characterized by a single relaxation time. This spread in relaxation times results from the fractal nature of the effective potential in which HAsO_4 and H_3AsO_4 groups in effect diffuse by means of intrabond proton transfer.^{20,21} This diffusion is responsible for the dielectric relaxation. As these groups cross potential barriers, the associated set of proton intrabond transfers can be called a cluster of pseudospins flips, in analogy with spin-glass behavior. Similar spreads in relaxation times have been seen in spin glasses²² where flipping of clusters of spins in the primary relaxation mechanism. As the temperature decreases below T_g there is a gradual increase in the distribution of relaxation times as is evident from the Cole-Cole plots in Fig. 5. A similar result was observed by Kutnjak *et al.*⁸ in DRADA with $x=0.25$ for the c -axis permittivity where they have used a Fröhlich-type distribution to analyze their dielectric results. For this ammonium concentration there is no ferroelectric transition. The distribution of relaxation times is greater in the undeuterated sample as can be seen from Fig. 5. To get the same shape for DRADA as for RADA we have to go about twice the temperature, just as to get to T_c in the pure crystal we have to go about twice as high a temperature. For a system with a single relaxation time the Cole-Cole plot would be a semicircle with its center on the ϵ'_a axis. The lowest-temperature plots in Fig. 5 probably deviate at the right-hand end from the circular shape shown because it is unlikely that the maximum ϵ'_a would suddenly increase at the lowest temperature.

Assuming that the temperatures corresponding to the peaks in $\epsilon''_a(T)$ in Figs. 3(d), 4(b) and 4(d) obey the exponential Arrhenius law

$$f = f_0 \exp(E_a / kT), \quad (2)$$

where f is the frequency, f_0 is the attempt frequency, and E_a is the activation energy, our results for the activation energy are summarized in Table I for $x=0.10$ RADA and 0.05 and 0.10 DRADA. The activation energy is greater in the case of the deuterated sample by almost a factor of 2. Here, $2E_a$ is approximately the energy required to create an HAsO_4 - H_3AsO_4 pair from two H_2AsO_4 groups.

Figure 6 shows the phase diagram for the undeuterated RADA family of proton glasses including data points from Ref. 7. In this diagram we point out that the coexistence (dotted) line extends to lower x values than suggested by Trybula *et al.*⁷ Data points for the 1-Hz T_g line in Fig. 6 have been obtained by extrapolating to 1 Hz in Figs. 3(a) and 4(a) for $x=0.05$ and 0.10, respectively.

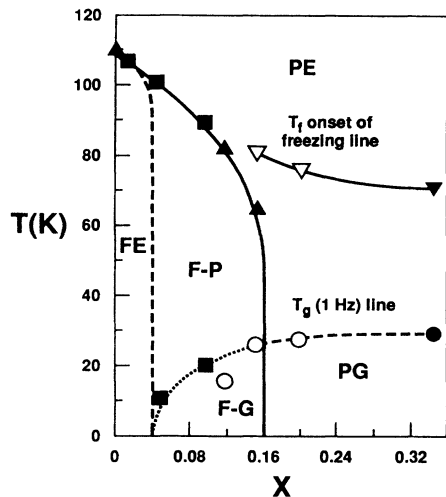


FIG. 6. The partial phase diagram of RADA as a function of fractional ammonium concentration x and temperature T . PE, FE, PG, FP, and FG denote paraelectric and ferroelectric phases, proton-glass regime, mixed ferroelectric-paraelectric and ferroelectric-proton-glass phases, respectively. The dotted line represents an extension from this work. The solid squares represent data from this work; other symbols represent data from Trybula *et al.* (Ref. 7).

CONCLUSIONS

We have investigated the dielectric response of RADA in the concentration range up to $x = 0.10$. Both the deuterated and undeuterated samples show proton-glass behavior for $x = 0.10$ and 0.05 . In the $x = 0.01$ undeuterated sample the ammonium concentration is too small to cause significant frustration between competing ferroelectric and antiferroelectric interactions. The dielectric response is seen to approach that of the pure sample as expected. So far there is no evidence for coexistence in the $x = 0.01$ sample.

This work extends our previous measurements⁷ to lower ammonium concentrations x and to deuterated crystals of RADA proton glass. The coexistence of proton-glass and ferroelectric phases found previously⁷ is shown to extend to lower x values than we expected. Three features noticed in the previous work⁷ are established more firmly: the height of the proton-glass contribution to ϵ'_a decreases with decreasing x , the steepness of the fall of ϵ'_a below T_c increases with decreasing x , and the maximum of ϵ'_a becomes more rounded with increasing x . We also established more securely the decrease in T_g with decreasing x , which we attribute to decreasing correlation length of proton-glass clusters intimately interlocked with ferroelectric clusters. Our Cole-Cole plots obtained in the audio-frequency range show the same flattening trend with decreasing temperature as those obtained by Kutnjak *et al.*⁸ in DRADA and by Brückner *et al.*²³ for RADP in the radio- to microwave-frequency range. While there is evidence of proton-glass behavior in the deuterated^{24,25} and undeuterated^{1,2} RADP crystals, it must be pointed out that coexistence of the ferroelectric phase with the paraelectric or proton-glass phase on the low x side of the phase diagram has still not been reported for these crystals. However, a dielectric behavior labeled "reentrant" by Takeshige *et al.*³ in $x = 0.75$ RADP is considered by us to indicate intimate coexistence of proton-glass and antiferroelectric regions. Further investigation in this coexistence region for the Rb and K phosphates and arsenates is needed to compare this phenomenon in KDP-type systems.

ACKNOWLEDGMENTS

The authors would like to thank Professor J. E. Drumheller for the loan of the apparatus used in the lowest temperature measurements, and Dr. S. L. Hutton for automating the dielectric measuring apparatus. This work was supported by National Science Foundation Grant No. DMR-9017429.

*On leave from University of North Dakota, Grand Forks, ND 58202.

¹E. Courtens, *J. Phys. (Paris) Lett.* **43**, L199 (1982).

²H. Terauchi, *Ferroelectrics* **64**, 87 (1985).

³M. Takashige, H. Terauchi, Y. Miura, and S. Hoshino, *J. Phys. Soc. Jpn.* **54**, 3250 (1985).

⁴S. Iida and H. Terauchi, *J. Phys. Soc. Jpn.* **52**, 4044 (1983).

⁵E. Courtens, *Helv. Phys. Acta*, **56**, 705 (1983).

⁶J. Eom, J. Yoon, and S. Kwun, *Phys. Rev. B* **44**, 2826 (1991).

⁷Z. Trybula, V. H. Schmidt, and J. E. Drumheller, *Phys. Rev. B* **43**, 1287 (1991).

⁸Z. Kutnjak, A. Levstik, C. Filipic, R. Pirc, B. Tadic, R. Blinc, H. Kabelka, A. Fuith, and H. Warhanek, *J. Phys.: Condens. Matter* **3**, 91 (1991).

⁹S. Kim and S. Kwun, *Phys. Rev. B* **42**, 638 (1990).

¹⁰J. P. DeLooze, B. MacG. Campbell, N. S. Dalal, and R. Blinc, *Physica B* **162**, 1 (1990).

¹¹Z. Trybula, V. H. Schmidt, J. E. Drumheller, D. He, and Z. Li, *Phys. Rev. B* **40**, 5289 (1989).

¹²K. Lee and N. Kim, *J. Phys. Soc. Jpn.* **57**, 1895 (1988).

¹³J. Kim, N. Kim, and K. Lee, *J. Phys. C* **21**, L663 (1988).

¹⁴Z. Trybula, J. Stankowski, L. Szczepanska, R. Blinc, Al. Weiss, and N. S. Dalal, *Ferroelectrics* **79**, 335 (1988); *Physica B* **153**, 143 (1988).

¹⁵W. T. Sobol, J. G. Cameron, M. M. Pintar, and R. Blinc, *Phys. Rev. B* **35**, 7299 (1987).

¹⁶L. N. Kamysheva, Yu. S. Zolototrubov, and S. A. Gridnev, *Ferroelectrics* **8**, 559 (1974).

¹⁷R. Blinc, M. Burgar, and A. Levstik, *Solid State Commun.* **12**, 573 (1973).

¹⁸R. J. Nelmes, *Ferroelectrics* **71**, 87 (1987).

¹⁹T. Nagamiya, *Prog. Theor. Phys. Jpn.* **7**, 275 (1952).

²⁰V. H. Schmidt, *J. Mol. Struct.* **177**, 257 (1988).

²¹V. H. Schmidt, *Ferroelectrics* **78**, 207 (1988).

²²D. Huser, L. E. Wenger, A. J. van Duynveldt, and J. A. Mydosh, *Phys. Rev. B* **27**, 3100 (1983).

²³H. J. Brückner, E. Courtens, and H.-G. Unruh, *Z. Phys. B* **73**, 337 (1988).

²⁴V. H. Schmidt, S. Waplak, S. Hutton, and P. Schnackenberg, *Phys. Rev. B* **30**, 2795 (1984).

²⁵E. Courtens, *Phys. Rev. B* **33**, 2975 (1986).